A new ordered phase in the spin-½ triangular antiferromagnetic system $CsCu_{1-x}Co_xCl_3$



2000 J. Phys.: Condens. Matter 12 975

(http://iopscience.iop.org/0953-8984/12/6/319)

J. Phys.: Condens. Matter **12** (2000) 975–984. Printed in the UK PII: S0953-8984(00)08525-8

# A new ordered phase in the spin-$\frac{1}{2}$ triangular antiferromagnetic system $CsCu_{1-x}Co_xCl_3$

T Ono, H Horai and H Tanaka

Department of Physics, Tokyo Institute of Technology, Oh-okayama 2-12-1, Meguro-ku, Tokyo 152-8551, Japan

Received 8 October 1999

**Abstract.** The magnetization and magnetic torque of the triangular antiferromagnetic system $CsCu_{1-x}Co_xCl_3$ with $x \leqslant 0.032$ have been measured in magnetic fields up to 7 T. $CsCuCl_3$ is a spin-$\frac{1}{2}$ triangular antiferromagnet with planar anisotropy, and has a 120° spin structure in the $c$-plane below $T_N = 10.5$ K. It is observed that the macroscopic anisotropy changes from the planar type to the axial one with increasing $Co^{2+}$ concentration $x$. It is found that the small amount of $Co^{2+}$ doping produces a new ordered phase in the low-temperature and low-field region, i.e., the present system can undergo two phase transitions at zero field. The transition field at which the new phase becomes unstable is minimum for $\boldsymbol{H} \parallel \boldsymbol{c}$ and maximum for $\boldsymbol{H} \perp \boldsymbol{c}$. With increasing $Co^{2+}$ concentration $x$, the area of the new phase is enlarged in the phase diagram for temperature versus magnetic field. The new phase has a weak spontaneous magnetization in the $c$-direction.

## 1. Introduction

Many hexagonal $ABX_3$ compounds crystallize in the $CsNiCl_3$ structure or ones closely related to it. When $B^{2+}$ ions are magnetic, they behave as triangular antiferromagnets (TAF) at low temperatures, and exhibit a wide variety of magnetic phases due to the bonding frustration in the $c$-plane and magnetic anisotropy [1]. $CsCuCl_3$ is one of the hexagonal $ABX_3$ compounds. Over the last few decades, $CsCuCl_3$ has attracted considerable attention on the basis of the structural phase transition and the magnetic properties.

Since the $Cu^{2+}$ ion is Jahn–Teller active, $CsCuCl_3$ undergoes a structural phase transition at $T_t = 423$ K. Below $T_t$, all $CuCl_6$ octahedra are elongated along one of the principal axes, and the longest axes form a helix along the $c$-axis with a repeat length of six [2–7]. The low-symmetric crystal structure can lead to the antisymmetric interaction of the Dzyaloshinsky–Moriya (D–M) type between the neighbouring spins in the $CuCl_6$ chain with the $D$-vector parallel to the $c$-axis. The exchange interactions in the chain and between the chains are ferromagnetic and antiferromagnetic, respectively [8, 9], and their values are $J_0/k_B = 28$ K and $J_1/k_B = -4.9$ K [10]. The magnetic anisotropy is of the planar type due to the pseudo-dipole interaction [10]. $CsCuCl_3$ undergoes a magnetic phase transition at $T_N = 10.5$ K at zero field [8,11–13]. In the ordered phase, spins lie in the $c$-plane and form the 120° structure, while along the $c$-axis, a long-period, i.e., about 72 layers of the $c$-plane, helical incommensurate structure is realized, due to the competition between the ferromagnetic interaction and the D–M interaction in the chain [8].

When the external field $\boldsymbol{H}$ is applied parallel to the $c$-axis, the spins tilt toward the $c$-axis to form an umbrella-type structure, as shown in figure 1(a). Within the mean-field theory, no phase transition is expected before saturation. However, Motokawa and co-workers [14] observed the

0953-8984/00/060975+10$30.00  

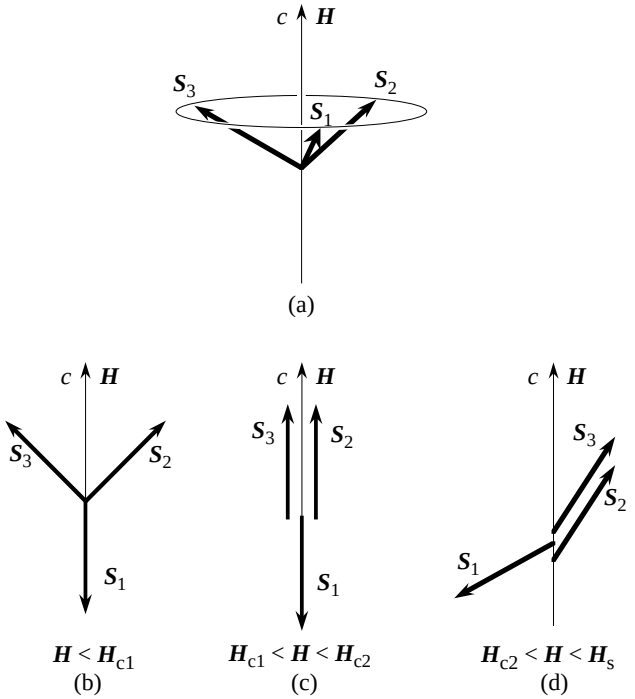


**Figure 1.** Various spin structures in magnetic fields for the ferromagnetically stacked and two-dimensional triangular Heisenberg antiferromagnet. (a) Umbrella-type structure, (b) low-field coplanar structure, (c) collinear structure and (d) high-field coplanar structure.

small magnetization jump at $H_c = 12.5$ T and $T = 1.1$ K for $\boldsymbol{H} \parallel \boldsymbol{c}$. Nikuni and Shiba [15] argued that the coplanar structure, as shown in figure 1(d), is stabilized in high magnetic fields due to the quantum fluctuation, so the transition from the umbrella-type structure to the coplanar structure shown in figure 1(d) can occur at $H_c$. The competition between the small planar anisotropy and the quantum fluctuation gives rise to the phase transition at $H_c$. The coplanar spin structure predicted for the high-field phase was confirmed by means of neutron scattering [16, 17] and ESR measurements [18] in pulsed high magnetic fields, and NMR measurements [19].

Using spin-wave approximation, Chubukov and Golosov [20] investigated the quantum effects on the spin ordering of the two-dimensional isotropic TAF in magnetic fields. They argued that with increasing magnetic field, the Heisenberg TAF undergoes a successive phase transition as shown in figures 1(b), 1(c) and 1(d) in that order. The intermediate collinear spin structure is stabilized in a finite field range $H_{c1} < H < H_{c2}$, where the critical fields $H_{c1}$ and $H_{c2}$ are a little smaller and greater than one-third of the saturation field $H_s$, respectively. Thus, the magnetization plateau is expected to be in the field range. However, such a successive phase transition is not observed in $CsCuCl_3$. We infer that the planar anisotropy which stabilizes the umbrella-type structure prevents the presence of the low-field coplanar and the intermediate collinear spin structures. If the planar anisotropy were reduced, the successive phase transition predicted by Chubukov and Golosov or an unexpected new phase might be observed. This is the motivation of our present study.

$CsCoCl_3$ is well known as a pseudospin-$\frac{1}{2}$ Ising TAF [21, 22]. Thus, we assume that, on average, $Co^{2+}$ ions substituting for $Cu^{2+}$ ions in $CsCu_{1-x}Co_xCl_3$ reduce the planar anisotropy.

In order to investigate the phase transitions in $CsCu_{1-x}Co_xCl_3$, we measured the temperature and field dependence of magnetizations for the samples with $0.015 \leqslant x \leqslant 0.032$. We also measured the magnetic torque to investigate the sign and the magnitude of the anisotropy. In this paper, we report the results.

## 2. Sample preparation and equipment

The crystals of $CsCu_{1-x}Co_xCl_3$ were prepared as follows: the source materials used were CsCl of 99% purity, $CuCl_2{\cdot}2H_2O$ of 99% purity and $CoCl_2{\cdot}6H_2O$ of 99% purity (Wako Pure Chemical Industries, Limited). In preparing $CsCuCl_3$, $CuCl_2{\cdot}2H_2O$ and CsCl were dehydrated separately by heating in vacuum for three days at $T \simeq 80$ °C and $T \simeq 150$ °C, respectively. After weighing, the samples were put into a quartz tube and dehydrated by heating in vacuum at $T \simeq 80$ °C for three days. In preparing $CsCoCl_3$, we first dissolved equimolar CsCl and $CoCl_2{\cdot}6H_2O$ in water and then vaporized the water by heating. The $CsCoCl_3$ powder obtained was put into a quartz tube and dehydrated by heating in vacuum at $T \simeq 200$ °C for three days. Single crystals of $CsCuCl_3$ and $CsCoCl_3$ were grown by the Bridgman technique from the melt. The temperature at the centre of the furnace was set at 550 °C for $CsCuCl_3$ and 650 °C for $CsCoCl_3$. Mixing single crystals of $CsCuCl_3$ and $CsCoCl_3$ in the ratio $1-x{:}x$, we prepared $CsCu_{1-x}Co_xCl_3$ by the Bridgman technique. Single crystals of size $\sim$1 cm$^3$ were obtained. The crystals are easily cleaved along the (1, 0, 0) plane. The crystals were cut into pieces weighing 50–100 mg for magnetic measurements. The concentration of the cobalt ions $x$ was analysed by emission spectrochemical analysis after the measurements were carried out. Since the resolution of the chemical analysis is higher than $1 \times 10^{-3}$ ppm, the reliability of the cobalt-ion concentration $x$ is $\pm 0.0001$.

The magnetization was measured down to 1.8 K in magnetic fields up to 7 T using a SQUID magnetometer (Quantum Design MPMS XL). The accuracy of the absolute value is approximately $5 \times 10^{-9}$ emu. A horizontal sample rotator was used to obtain the magnetization for various field directions.

The magnetic torque was measured using a torque meter (Yasunami YMT-H1) and an electromagnet. The torque meter used is an electric current-to-torque transducer-type one constructed for measuring torque values as small as $10^{-4}$–$10^{-3}$ dyn cm. We measure the current which generates counter-torque for keeping the orientation of the sample unchanged. The accuracy of the absolute value is approximately $1 \times 10^{-7}$ emu and that of the relative value is 1%. The sample was placed such that the external field always lies in the (1, 1, 0) plane containing the $c$-axis. The electromagnet was rotated at the rate of 1.5° s$^{-1}$ for the measurements of torque curves.

## 3. Results and discussion

Figure 2 shows the magnetization process for the sample with $x = 0.032$ at various temperatures. The external field is applied parallel to the $c$-axis. For $T = 1.8$ K, the magnetization jumps at $H_c = 3.6$ T. The field at which there is an inflection point in the magnetization is assigned to the transition field. The transition field $H_c$ decreases with increasing temperature. We observe the presence of a small spontaneous magnetization for $H < H_c$, which is also confirmed by the torque measurements, as discussed below. The magnitude of the spontaneous magnetization $M_s$ at $T = 1.8$ K is estimated by extrapolating the magnetization curve in the field region of $1.5\ \text{T} \leqslant H \leqslant 3.3$ T to zero (dotted line) as $M_s \simeq 2.5 \times 10^{-3}\ \mu_B$/atom.

The temperature dependence of the magnetization for $\boldsymbol{H} \parallel \boldsymbol{c}$ for the sample with $x = 0.032$

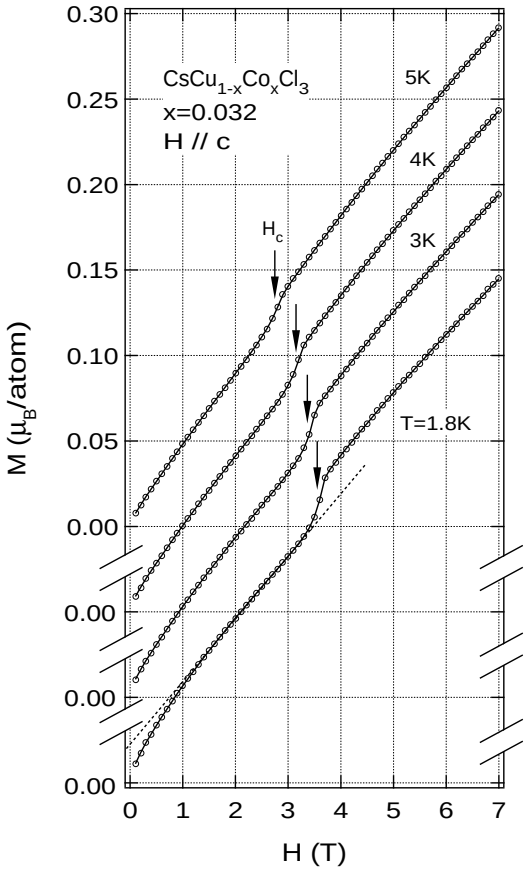


**Figure 2.** Field dependences of the magnetization for the sample with $x = 0.032$ at various temperatures. The external field is applied parallel to the $c$-axis. Transition fields are indicated by arrows. The dotted line through the data for $T = 1.8$ K denotes the extrapolation of the magnetization curve in the region 1.5 T $\leqslant H \leqslant$ 3.3 T to zero.

is shown in figure 3. The small anomaly at $T = 12$ K is due to an instrumental problem. When the applied field is higher than 4 T, a single phase transition occurs at $T_{N1} \simeq 9.5$ K, and the transition temperature is almost independent of the external field. On the other hand, for $H \leqslant 3$ T, we can see another anomaly on the low-temperature side, which is indicative of the second phase transition. In figure 3, the temperature at which $\mathrm{d}M/\mathrm{d}T$ gives the local maximum is assigned to the transition temperature $T_{N2}$. The transition temperature $T_{N2}$ shifts rapidly to the high-temperature side with decreasing external field. Sharp anomalies due to the phase transitions indicate good homogeneity of the sample.

The phase transition data for the samples with $x = 0.015$, 0.023 and 0.032 are summarized in figure 4. In this figure, open circles, triangles and closed circles indicate the transition points for the samples with $x = 0.015$, 0.023 and 0.032, respectively. We label each phase as shown in figure 4. With increasing $x$, the phase boundary between the paramagnetic phase and phase I shifts toward the low-temperature side. On the other hand, the area of phase II becomes enlarged with increasing $x$. For the sample with $x = 0.005$, we could not observe phase II. Thus, we infer that there exists a critical concentration $x_c$ for producing phase II. In the area of phase I, we could not detect any anomalies indicative of the phase transition in the

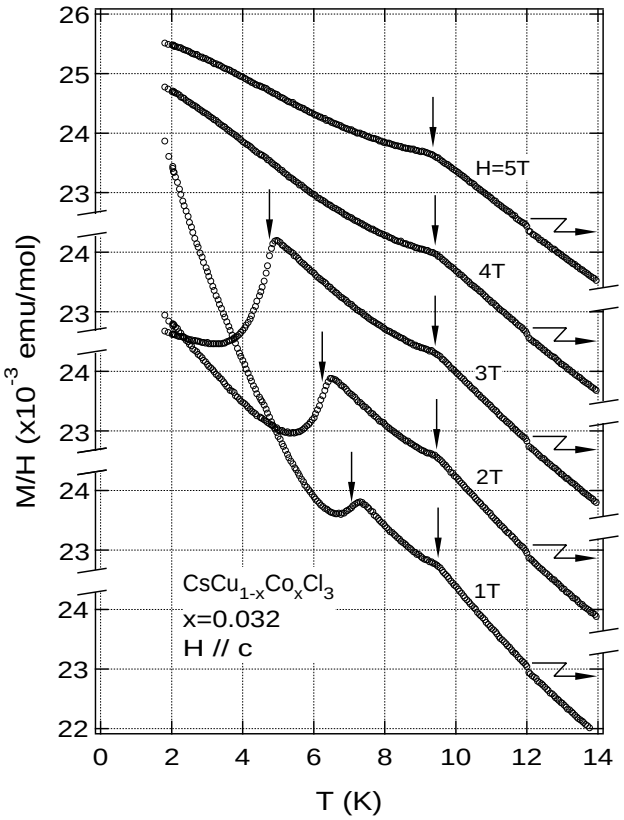


**Figure 3.** Temperature variations of the magnetization for $x = 0.032$ at the various external fields parallel to the $c$-axis. Transition temperatures are indicated by arrows.

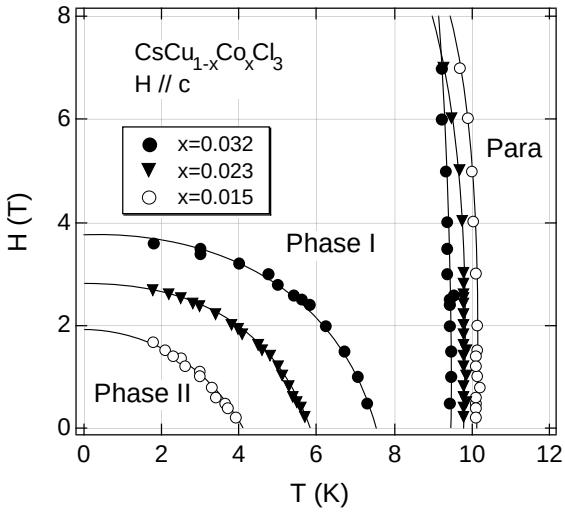


**Figure 4.** The magnetic phase diagram of $CsCu_{1-x}Co_xCl_3$ for the magnetic field parallel to the $c$-axis. Open circles, triangles and closed circles correspond to the transition points for $x = 0.015$, 0.023 and 0.032, respectively.

magnetization data.

We measured magnetization curves at various field directions for the sample with $x = 0.03$. The $\mathrm{d}M/\mathrm{d}H$ versus $H$ curves obtained at $T = 1.8$ K are shown in figure 5, where $\theta$ denotes the angle between the external field and the $c$-axis. The value of $\mathrm{d}M/\mathrm{d}H$ at around zero field is maximum at $\theta = 0^\circ$, and decreases with increasing $|\theta|$. This indicates that the steep increase of the magnetization near zero field for $\boldsymbol{H} \parallel \boldsymbol{c}$ is attributable not to the paramagnetic impurity, but to the small spontaneous magnetization along the $c$-axis. The transition from phase II to phase I can be observed at the peak position of $\mathrm{d}M/\mathrm{d}H$. Figure 6 shows the transition field $H_\mathrm{c}$ as a function of the angle $\theta$. The solid line is a visual guide. We can observe that the transition field $H_\mathrm{c}$ changes continuously with $\theta$, and has a minimum at $\theta = 0^\circ$ ($\boldsymbol{H} \parallel \boldsymbol{c}$) and a maximum at $\theta = \pm 90^\circ$ ($\boldsymbol{H} \perp \boldsymbol{c}$). If the transition field $H_\mathrm{c}$ is determined by the $c$-axis component of the external field, $H_\mathrm{c}$ is proportional to $1/\cos\theta$. However, the transition field obtained for $\boldsymbol{H} \perp \boldsymbol{c}$ is finite. This finding indicates that the field components parallel and perpendicular to the $c$-axis are both responsible for the phase transition.

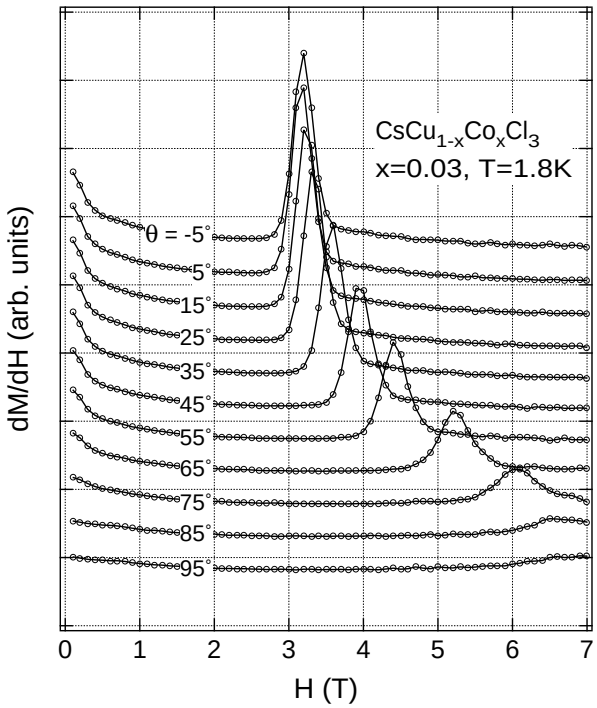


**Figure 5.** $\mathrm{d}M/\mathrm{d}H$ versus $H$ measured in various field directions and at 1.8 K for $x = 0.03$. $\theta$ denotes the angle between the external field and the $c$-axis.

The magnetic torque $L(\theta)$ is given by $L(\theta) = -\partial F/\partial\theta$, where $F$ is the free energy of the system and $\theta$ is the angle between the external field $H$ and the $c$-axis. When the torque $L(\theta)$ is proportional to $H^2 \sin 2\theta$, which is satisfied in the paramagnetic phase, $L(\theta)$ is expressed as

$$L(\theta) = -\frac{\partial F}{\partial \theta} = -\frac{1}{2}(\chi_\parallel - \chi_\perp)H^2 \sin 2\theta \tag{1}$$

where $\chi_\parallel$ and $\chi_\perp$ are the susceptibilities for $\boldsymbol{H} \parallel \boldsymbol{c}$ and $\boldsymbol{H} \perp \boldsymbol{c}$, respectively. Thus, we can obtain the difference of the susceptibilities $\chi_\parallel - \chi_\perp$ through the torque measurement.

Figure 7 shows the torque curves for $CsCuCl_3$ and $CsCu_{1-x}Co_xCl_3$ with $x = 0.015$,

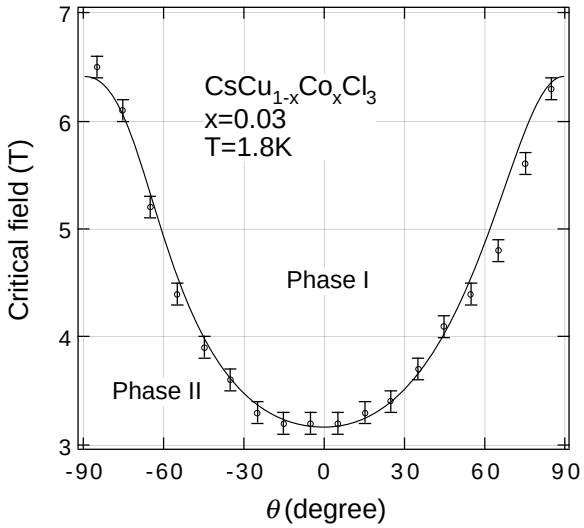


**Figure 6.** The angular dependence of the transition field $H_c$ measured at 1.8 K for $x = 0.03$. The solid line is a visual guide.

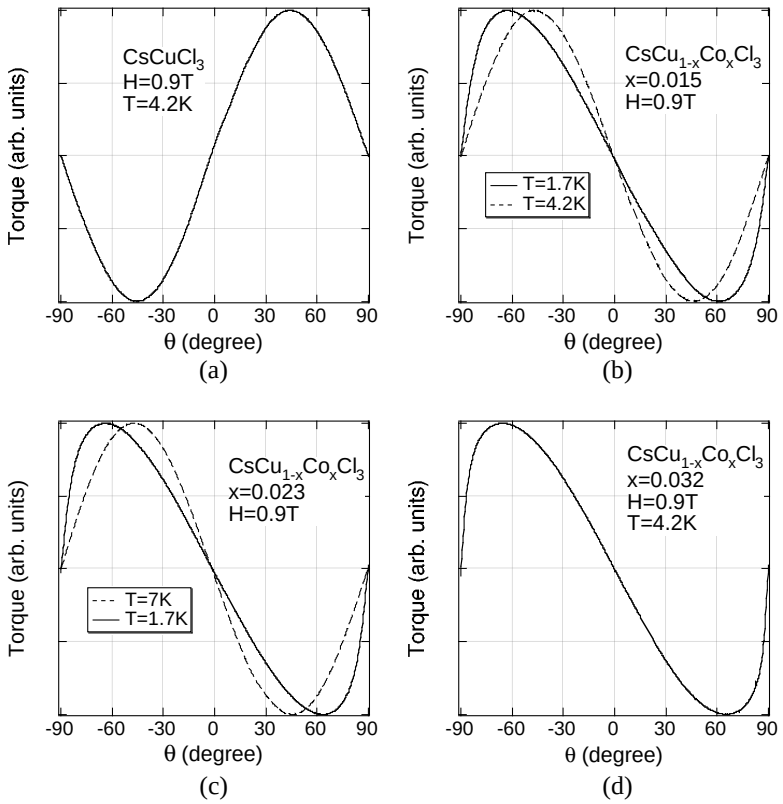


**Figure 7.** Torque curves for $CsCuCl_3$ and $CsCu_{1-x}Co_xCl_3$ with $x = 0.015$, 0.023 and 0.032. The external field of 0.9 T is rotated in the *ac*-plane. In (b) and (c), solid and dashed lines denote the torque curves in phase II and phase I, respectively.

0.023 and 0.032. The external field of $H = 0.9$ T is applied. The dashed and solid curves for $CsCu_{1-x}Co_xCl_3$ are the torque curves in phase I and phase II, respectively. The magnetic torques for $CsCuCl_3$ and those in phase I for $x = 0.015$ and 0.023 are proportional to $H^2 \sin 2\theta$. From the torque curve, we see $\chi_{\parallel} < \chi_{\perp}$ in the ordered phase of $CsCuCl_3$. On the other hand, for $x = 0.015$ and 0.023, $\chi_{\parallel} > \chi_{\perp}$ in phase I. In phase II, the peak of the torque curve shifts toward $\theta = \pm 90^{\circ}$, and the curve resembles the letter 'N'. The torque curve can be understood in terms of the small spontaneous magnetization parallel to the $c$-axis, which produces the torque proportional to $-H \sin\theta$ for $-90^{\circ} \leqslant \theta \leqslant 90^{\circ}$. The spontaneous magnetization does not exist in phase I, because the torque is described by equation (1).

Figure 8 shows the temperature dependence of $\Delta\chi$ defined by

$$\Delta\chi = -2L(\theta = 45^{\circ})/H^2. \tag{2}$$

The data were collected at $H = 0.5$ T and 0.3 T for $CsCu_{1-x}Co_xCl_3$ and $CsCuCl_3$, respectively. In the paramagnetic phase in which the torque is proportional to $H^2 \sin 2\theta$, $\Delta\chi$ is equal to $\chi_{\parallel} - \chi_{\perp}$. Phase transitions are detected at almost the same temperatures as those observed in the magnetization measurements. In the paramagnetic phase, $\Delta\chi$ changes its sign from minus

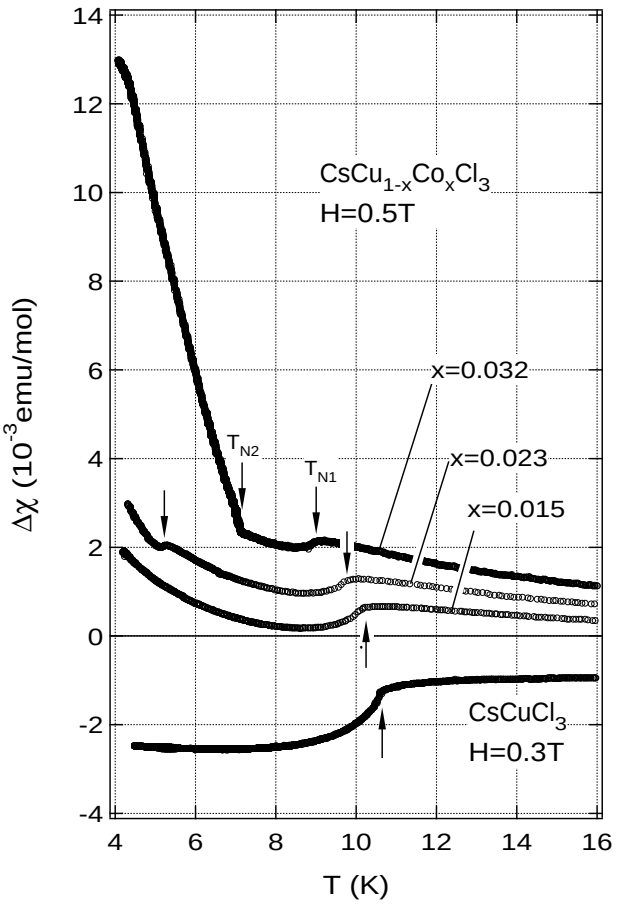


**Figure 8.** Temperature dependences of $\Delta\chi$ defined by equation (2), for $CsCuCl_3$ and for $CsCu_{1-x}Co_xCl_3$ with $x = 0.015$, 0.023 and 0.032 in the phase transition region. Transition points are indicated by arrows.

to plus with increasing $x$, and its magnitude increases. It is considered that $\Delta\chi$ in the paramagnetic phase is almost proportional to the anisotropy, because the difference between the $g$-factors parallel and perpendicular to the $c$-axis is small in $CsCuCl_3$, i.e., $g_\perp - g_\parallel \simeq 0.02$ [18,23]. Therefore, the present result indicates that, on average, with increasing $x$, the anisotropy changes from a planar type to an axial one and that phase II appears when the anisotropy is of the axial type.

The spin structure of phase II is stabilized with the help of the axial anisotropy. With decreasing $Co^{2+}$ concentration $x$, the area of phase II is reduced and then disappears. Thus, it is logical to deduce that phase I which surrounds phase II is essentially identical to the ordered phase of $CsCuCl_3$. Since the quantity of $Co^{2+}$ ions is small, we assume that the exchange interactions in the chain and between the chains are not greatly modified. Since the intrachain interaction is ferromagnetic, the spin-flop transition cannot be expected. If the coplanar structure shown in figure 1(b) is realized in phase II, the transition at $H_c$ for $\boldsymbol{H} \parallel \boldsymbol{c}$ is not understandable, because both the anisotropy and the quantum fluctuation in high fields favour the coplanar structure over the umbrella-type one [15]. At present, the spin structure of phase II is unknown. Neutron scattering experiments are needed to elucidate the spin structures of phase I and II and the mechanisms which lead to the phase transitions in the present system.

## 4. Conclusions

We measured the magnetization and magnetic torque of the triangular antiferromagnetic system $CsCu_{1-x}Co_xCl_3$ with $x \leqslant 0.032$, in which $Co^{2+}$ ions were described as having pseudospin $\frac{1}{2}$ substitute for $Cu^{2+}$ ions. With increasing $Co^{2+}$ concentration $x$, the magnetic anisotropy changes from planar type to axial in the region $0 < x < 0.015$, and its magnitude increases. For the sample with $x = 0.005$, which seems to be closely isotropic, any field-induced phase transition was observed below 7 T. It was found that for $0.015 \leqslant x \leqslant 0.032$, a new ordered phase (II) appears in the low-temperature and low-field region of an ordered phase (I) which is assumed to be identical to the ordered phase of $CsCuCl_3$ (see the schematic phase diagram in figure 7). With increasing $Co^{2+}$ concentration $x$, the area of the new phase becomes enlarged in the phase diagram. The transition field at which the new phase becomes unstable is minimum for $\boldsymbol{H} \parallel \boldsymbol{c}$ and maximum for $\boldsymbol{H} \perp \boldsymbol{c}$. The new phase has weak spontaneous magnetization along the $c$-direction. The spin structure of the new phase is unknown.

## References


[1] Collins M F and Petrenko O A 1997 *Can. J. Phys.* **75** 605 and references therein
[2] Schlueter A W, Jacobson R A and Rundle R E 1966 *Inorg. Chem.* **5** 277
[3] Kroese C J, Maaskant W J A and Verschoor G D 1974 *Acta Crystallogr.* B **30** 1053
[4] Hirotsu S 1977 *J. Phys.: Condens. Matter* **10** 967
[5] Laiho R, Natarajan N and Kaira M 1973 *Phys. Status Solidi* a **15** 311
[6] Graf H A, Shirane G, Schotte U, Dachs H, Pyka N and Iizumi M 1989 *J. Phys.: Condens. Matter* **1** 3743
[7] Schotte U, Graf H A and Dachs H 1989 *J. Phys.: Condens. Matter* **1** 3765
[8] Adachi K, Achiwa N and Mekata M 1980 *J. Phys. Soc. Japan* **49** 545
[9] Tazuke Y, Tanaka H, Iio K and Nagata K 1981 *J. Phys. Soc. Japan* **50** 3919
[10] Tanaka H, Schotte U and Schotte K D 1992 *J. Phys. Soc. Japan* **61** 1344
[11] Rioux F J and Gerstein B C 1969 *J. Chem. Phys.* **50** 758
[12] Hyodo H, Iio K and Nagata K 1981 *J. Phys. Soc. Japan* **50** 1545
[13] Weber H B, Werner T, Wosnitza J, von Löhneysen H and Schotte U 1996 *Phys. Rev.* B **54** 15 924
[14] Nojiri H, Tokunaga Y and Motokawa M 1988 *J. Physique Coll.* **49** C8 1459
[15] Nikuni T and Shiba H 1993 *J. Phys. Soc. Japan* **62** 3268
[16] Mino M, Ubukata K, Bokui T, Arai M, Tanaka H and Motokawa M 1994 *Physica* B **201** 213

[17] Schotte U, Stüsser N, Schotte K D, Weinfurter H, Mayer H M and Winkelmann M 1994 *J. Phys.: Condens. Matter* **6** 10 105
[18] Ohta H, Imagawa S, Motokawa M and Tanaka H 1993 *J. Phys. Soc. Japan* **62** 3011
[19] Chiba M, Ohara K, Ajiro Y and Morimoto T 1993 *J. Phys. Soc. Japan* **62** 4186
[20] Chubukov A V and Golosov D I 1991 *J. Phys.: Condens. Matter* **3** 69
[21] Mekata M 1977 *J. Phys. Soc. Japan* **42** 76
[22] Mekata M and Adachi K1978 *J. Phys. Soc. Japan* **44** 806
[23] Tanaka H, Iio K and Nagata K 1985 *J. Phys. Soc. Japan* **54** 4345